



Contents lists available at ScienceDirect

# Journal of Computational and Applied Mathematics

journal homepage: [www.elsevier.com/locate/cam](http://www.elsevier.com/locate/cam)

## Immersed finite element methods for unbounded interface problems with periodic structures<sup>☆</sup>

Yong Cao<sup>a</sup>, Yuchuan Chu<sup>a</sup>, Xiaoshi Zhang<sup>b</sup>, Xu Zhang<sup>c,\*</sup><sup>a</sup> Department of Mechanical Engineering & Automation, Harbin Institute of Technology, Shenzhen Graduate School, Shenzhen, Guangdong 518055, PR China<sup>b</sup> Department of Natural Sciences & Humanities, Harbin Institute of Technology, Shenzhen Graduate School, Shenzhen, Guangdong 518055, PR China<sup>c</sup> Department of Mathematics, Purdue University, West Lafayette, IN 47907, USA

### ARTICLE INFO

#### Article history:

Received 1 August 2015

Received in revised form 15 April 2016

#### Keywords:

Periodic boundary condition

Immersed finite element

Unbounded interface problem

Periodic structures

Electrostatic field

### ABSTRACT

Interface problems arise in many physical and engineering simulations involving multiple materials. Periodic structures often appear in simulations with large or even unbounded domain, such as magnetostatic/electrostatic field simulations. Immersed finite element (IFE) methods are efficient tools to solve interface problems on a Cartesian mesh, which is desirable to many applications like particle-in-cell simulation of plasma physics. In this article, we develop an IFE method for an interface problem with periodic structure on an infinite domain. To cope with the periodic boundary condition, we modify the stiffness matrix of the IFE method. The new matrix is maintained symmetric positive definite, so that the linear system can be solved efficiently. Numerical examples are provided to demonstrate features of this method.

© 2016 Elsevier B.V. All rights reserved.

### 1. Introduction

In engineering simulations, many devices characterize highly regular extended periodic structures, such as optics system in ion thruster [1,2]. Numerical methods are usually applicable when such infinite samples possess a periodicity known *a priori*. In the mean time, only finite regions of these infinite structures are of practical interest. Simulation on a finite region is usually computationally feasible through existing numerical methods. One frequently used approach is to model only a small part of the infinite sample by truncating outer boundaries. This approach often assumes the normal derivative of the potential to be zero at the periodic boundaries. For example, the homogeneous Neumann boundary condition is enforced in the simulation of spacecraft–ion thruster interaction in [1]. However, the normal derivative of the potential is continuous at the periodic boundary edges but not necessary to be zero. For electromagnetic field problems, such as plasma–environment interaction simulation, periodic boundary conditions (PBC) are an important tool to understand the behavior of periodic structures. Many techniques have been developed in the study of PBC, and they have been used extensively in the simulation of periodical electromagnetic fields [3–6].

To simulate the behaviors of plasma medium, the particle-in-cell (PIC) method [7–10] models plasma as many macro-particles and follows the evolution of the orbits of individual particles in the self-consistent electromagnetic field. This

<sup>☆</sup> This work is supported by the National Science Foundation of China (10875034, 11175052).

\* Corresponding author.

E-mail addresses: [yongc@hitsz.edu.cn](mailto:yongc@hitsz.edu.cn) (Y. Cao), [yuchuan.chu@hitsz.edu.cn](mailto:yuchuan.chu@hitsz.edu.cn) (Y. Chu), [xishzhang@gmail.com](mailto:xishzhang@gmail.com) (X. Zhang), [xuzhang@purdue.edu](mailto:xuzhang@purdue.edu) (X. Zhang).<http://dx.doi.org/10.1016/j.cam.2016.04.020>

0377-0427/© 2016 Elsevier B.V. All rights reserved.

method includes two main processes which are often called “scatter” (for finding the charge density from the particle positions) and “gather” (for interpolating the particle forces from the potential at the grid points). The PIC method is difficult to be utilized with body-fitting meshes, because locating millions of particles in an unstructured grid costs significant searching time in both “gather” and “scatter” steps in a typical PIC computational cycle; hence, it is preferable to use a more structured mesh to fulfil the process via indexing with the coordinates. Moreover, media materials in a PIC method are often separated by an interface with complicated geometry (see [9,11,12]). As a result, it is unrealistic to expect optimal convergent solution in a structured non-body-fitting mesh simply by conventional finite element methods.

Recently, a new type of field solvers, named immersed finite element (IFE) methods [13–20] have been developed to solve interface problems based on Cartesian meshes. In an IFE method, material interfaces are allowed to cut through some elements which are called interface elements, distinguished from those non-interface elements which are disjoint from interfaces. Standard finite element basis functions are adopted on non-interface elements, and piecewise polynomials are used to construct special IFE basis function on interface elements to mimic the behavior of the exact solution. For interface problems with nonhomogeneous flux jump conditions, a homogenization with the level set method was developed in [21]. Alternatively, the local IFE space can be enriched by adding a basis function that can capture the nonhomogeneous flux jump [22]. Recently, this idea was extended to solve a moving interface problem with nonhomogeneous flux jump [23]. We refer to [24] for IFE methods in handling nonhomogeneous jump for both solution and flux.

In this article, we will propose an IFE method for solving an unbounded interface problem with periodic structure. To simulate the behavior in a finite domain, we truncate the unbounded domain and impose appropriate PBC. We will modify the global stiffness matrix to accommodate the PBC. Such modification is only carried out in the periodic variation domain. The new global matrix is preserved symmetric positive definite, so that the linear system can be solved efficiently.

The rest of this article is organized as follows. In Section 2, we introduce the unbounded interface problem and develop an IFE method for the truncated problem with PBC. In Section 3, we present the matrix modification technique to accommodate PBC. Numerical examples and some related discussion are provided in Section 4. Finally, in Section 5 we draw some conclusions.

## 2. IFE methods for interface problems

In this section, we will first present the unbounded elliptic interface problem and the truncated model problem with periodic boundary condition in a finite domain. Next we will recall some IFE methods for elliptic interface problem with homogeneous [25] and nonhomogeneous flux jump [22]. To make our presentation concise, we only consider the bilinear IFE methods based on rectangular meshes in the article. For linear IFE methods on triangular meshes, the discussion is similar and we refer readers to [26,27] for more details.

### 2.1. An unbounded elliptic interface problem

Let  $\hat{\Omega} = (-\infty, \infty) \times (0, 1)$  be an unbounded (in  $x$ -direction) domain. A smooth interface curve  $\hat{\Gamma}$  separates  $\hat{\Omega}$  into sub-domains  $\hat{\Omega}^-$  and  $\hat{\Omega}^+$ . We consider the following second-order elliptic interface problem

$$-\nabla \cdot (\beta \nabla u) = f \quad \text{in } \hat{\Omega}^+ \cup \hat{\Omega}^-. \quad (2.1)$$

Assume that the solution  $u$  has the periodic structure in the  $x$ -direction, i.e., there is a positive constant  $L$  such that

$$u(x, y) = u(x + L, y), \quad \forall x \in (-\infty, \infty). \quad (2.2)$$

In  $y$ -direction, we assume that the solution satisfies the Dirichlet boundary condition

$$u(x, 0) = g_0(x), \quad (2.3)$$

$$u(x, 1) = g_1(x). \quad (2.4)$$

Across the interface  $\hat{\Gamma}$ , the solution is assumed to satisfy the interface jump conditions

$$[[u]]_{\hat{\Gamma}} = 0, \quad (2.5)$$

$$\left[ \left[ \beta \frac{\partial u}{\partial n} \right] \right]_{\hat{\Gamma}} = Q. \quad (2.6)$$

Here  $[[v]]_{\hat{\Gamma}} = (v|_{\hat{\Omega}^+})_{\hat{\Gamma}} - (v|_{\hat{\Omega}^-})_{\hat{\Gamma}}$  is the jump of  $v$  across  $\hat{\Gamma}$ . The function  $Q$  is the jump of normal flux, and  $n$  is the unit normal vector of  $\hat{\Gamma}$ . The flux jump is said to be homogeneous if  $Q = 0$ ; otherwise it is nonhomogeneous. Also, we assume that the coefficient function  $\beta$  is periodic in the  $x$ -direction of periodicity  $L$ . Without loss of generality, the coefficient  $\beta(x, y)$  is discontinuous across the interface  $\hat{\Gamma}$ . For simplicity, we assume that  $\beta$  is a piecewise constant function as follows:

$$\beta(x, y) = \begin{cases} \beta^-, & (x, y) \in \hat{\Omega}^-, \\ \beta^+, & (x, y) \in \hat{\Omega}^+. \end{cases}$$

Applying a homogenization technique can change the nonhomogeneous Dirichlet boundary conditions (2.3) and (2.4) to homogeneous. Thus, without loss of generality, we assume  $g_0 = g_1 = 0$  in the following discussion.

The model problem (2.1)–(2.6) is defined on an unbounded domain. Due to its periodic structure, we can simulate the behavior of this model problem in a finite domain by truncating outer boundary of  $\hat{\Omega}$ , and imposing appropriate periodic boundary conditions. To be more specific, we consider a finite rectangular domain  $\Omega = (0, L) \times (0, 1)$ , and denote the truncated interface by  $\Gamma = \hat{\Gamma} \cap \Omega$ . The truncated interface  $\Gamma$  separates the domain  $\Omega$  into two parts  $\Omega^+$  and  $\Omega^-$  such that  $\Omega = \Omega^+ \cup \Omega^- \cup \Gamma$ . We also denote the top, bottom, left, right boundaries of  $\Omega$  by  $\Gamma_t$ ,  $\Gamma_b$ ,  $\Gamma_l$ , and  $\Gamma_r$ , respectively. The interface problem (2.1)–(2.6) can be reformulated in a finite domain.

$$-\nabla \cdot (\beta \nabla u) = f \quad \text{in } \Omega^+ \cup \Omega^-, \quad (2.7)$$

$$u(0, y) = u(L, y), \quad \beta \frac{\partial u}{\partial n}(0, y) = \beta \frac{\partial u}{\partial n}(L, y) \quad \text{on } \Gamma_l \cup \Gamma_r, \quad (2.8)$$

$$u(x, 0) = u(x, 1) = 0 \quad \text{on } \Gamma_t \cup \Gamma_b, \quad (2.9)$$

$$\llbracket u \rrbracket_\Gamma = 0, \quad \left[ \left[ \beta \frac{\partial u}{\partial n} \right] \right]_\Gamma = Q(x, y) \quad \text{on } \Gamma. \quad (2.10)$$

The problem (2.7)–(2.10) is an elliptic interface problem with periodic boundary conditions and nonhomogeneous flux jump. We refer to [28] for the well-posedness of elliptic problems with periodic boundary conditions.

## 2.2. IFE approximation for homogeneous flux jump

We first recall the bilinear IFE method [25,29] for interface problem with homogeneous flux jump, i.e.,  $Q = 0$  in (2.10).

Assume that  $\mathcal{T}_h = \{T\}$  is a uniform rectangular mesh of the truncated domain  $\Omega$  with mesh size  $h$ . If an element  $T$  is cut by the truncated interface  $\Gamma$ , it is called an interface element; otherwise, it is called a non-interface element. The sets of all interface elements and non-interface elements are denoted by  $\mathcal{T}_h^{int}$ , and  $\mathcal{T}_h^{non}$ , respectively. For a typical interface rectangle  $T$  with vertices  $A_i$ ,  $i = 1, 2, 3, 4$ , the interface  $\Gamma$  is assumed to intersect  $T$  at two distinct points, denoted by  $D$  and  $E$ . The line segment  $\overline{DE}$  is used to approximate the physical interface curve  $\Gamma \cap T$ , and the line  $\overline{DE}$  divides  $T$  into two sub-elements, denoted by  $T^+$  and  $T^-$ . The local bilinear IFE nodal basis functions  $\phi_{i,T}$ ,  $i = 1, 2, 3, 4$  have the following form:

$$\phi_{i,T}(x, y) = \begin{cases} \phi_{i,T}^-(x, y) = a_i^- + b_i^-x + c_i^-y + d_i^-xy, & (x, y) \in T^-, \\ \phi_{i,T}^+(x, y) = a_i^+ + b_i^+x + c_i^+y + d_i^+xy, & (x, y) \in T^+. \end{cases} \quad (2.11)$$

These local IFE basis functions satisfy the following constraints:

### 1. nodal values restrictions

$$\phi_{i,T}(A_j) = \delta_{ij}, \quad i, j = 1, 2, 3, 4, \quad (2.12)$$

### 2. continuity on $\overline{DE}$

$$\phi_{i,T}^+(D) = \phi_{i,T}^-(D), \quad \phi_{i,T}^+(E) = \phi_{i,T}^-(E), \quad d_i^+ = d_i^-, \quad i = 1, 2, 3, 4, \quad (2.13)$$

### 3. weak continuity of normal flux

$$\int_{\overline{DE}} \left( \beta^- \frac{\partial \phi_{i,T}^-}{\partial n} - \beta^+ \frac{\partial \phi_{i,T}^+}{\partial n} \right) ds = 0, \quad i = 1, 2, 3, 4, \quad (2.14)$$

where the normal  $n$  is a unit normal vector to the line segment  $\overline{DE}$ .

In [25], it was shown that the conditions (2.12)–(2.14) uniquely determine a set of nodal IFE basis functions  $\phi_{i,T}$ ,  $i = 1, 2, 3, 4$  on the interface element  $T$ . The local bilinear IFE space  $S_h(T)$  on an interface element  $T \in \mathcal{T}_h^{int}$  is defined as

$$S_h(T) = \text{span}\{\phi_{1,T}, \phi_{2,T}, \phi_{3,T}, \phi_{4,T}\}. \quad (2.15)$$

Denote the set of nodes on  $\mathcal{T}_h$  by  $\mathcal{N}_h$ . The set of nodes not on  $\Gamma_t$  and  $\Gamma_b$  is denoted by  $\hat{\mathcal{N}}_h$  and the number of nodes in  $\hat{\mathcal{N}}_h$  is called  $N$ . On each node  $(x_i, y_i)$ ,  $i = 1, \dots, N$ , we define the global bilinear IFE basis function  $\Phi_i$  such that

$$\Phi_i(x_j, y_j) = \delta_{ij}, \quad \forall (x_j, y_j) \in \hat{\mathcal{N}}_h,$$

and

$$\Phi_i|_T \in S_h(T), \quad \forall T \in \mathcal{T}_h^{int}, \quad \text{and} \quad \Phi_i|_T \in \mathbb{Q}_1(T) \quad \forall T \in \mathcal{T}_h^{non}.$$

Here,  $\mathbb{Q}_1(T) = \text{span}\{1, x, y, xy\}$  is standard bilinear polynomial space. Finally, the global bilinear IFE space can be formed as  $S_h(\Omega) = \text{span}\{\Phi_i : i = 1, 2, \dots, N\}$ . We refer readers to [30,25,31–33] for more details about bilinear IFE methods for homogeneous flux jump.

### 2.3. IFE approximation for nonhomogeneous flux jump

To handle the nonhomogeneous flux jump, the local IFE space  $S_h(T)$  is enriched by adding another basis  $\phi_{J,T}$  (see [30, 22]). The function  $\phi_{J,T}$  is of the form

$$\phi_{J,T}(x, y) = \begin{cases} \phi_{J,T}^-(x, y) = a_j^- + b_j^-x + c_j^-y + d_j^-xy, & (x, y) \in T^-, \\ \phi_{J,T}^+(x, y) = a_j^+ + b_j^+x + c_j^+y + d_j^+xy, & (x, y) \in T^+, \end{cases} \quad (2.16)$$

and satisfies

1. zero nodal value restrictions

$$\phi_{J,T}(A_j) = 0, \quad j = 1, 2, 3, 4, \quad (2.17)$$

2. continuity on  $\overline{DE}$

$$\phi_{J,T}^+(D) = \phi_{J,T}^-(D), \quad \phi_{J,T}^+(E) = \phi_{J,T}^-(E), \quad d_j^+ = d_j^-, \quad (2.18)$$

3. unit flux jump

$$\int_{\overline{DE}} \left( \beta^- \frac{\partial \phi_{J,T}^-}{\partial n} - \beta^+ \frac{\partial \phi_{J,T}^+}{\partial n} \right) ds = 1, \quad (2.19)$$

where  $n$  is the unit normal vector to the line segment  $\overline{DE}$ .

Again, conditions (2.17)–(2.19) uniquely determine the basis  $\phi_{J,T}$  [22], and each  $\phi_{J,T}$  is supported only on the interface element  $T$ . Finally, the IFE space for nonhomogeneous flux can be defined as

$$S_h^{IFE}(\Omega) = S_h(\Omega) \oplus \text{span}\{\phi_{J,T} : \forall T \in \mathcal{T}_h^{int}\}. \quad (2.20)$$

The approximation property of this IFE space  $S_h^{IFE}(\Omega)$  has been considered in [22] by the nodal value interpolation. The exact solution  $u$  of (2.7)–(2.10) is included in the following Sobolev space

$$H_{\beta,Q}^2(\Omega) = \left\{ u \in H^1(\Omega) : u|_{\Omega^s} \in H^2(\Omega^s), s = \pm, \left[ \left[ \beta \frac{\partial u}{\partial n} \right] \right] = Q \right\}. \quad (2.21)$$

Here  $n_\Gamma$  is the unit normal vector at the interface curve  $\Gamma$  pointing from  $\Omega^+$  to  $\Omega^-$ . The interpolation operator  $I_h : H_{\beta,Q}^2(\Omega) \rightarrow S_h^{IFE}(\Omega)$  is defined by

$$I_h u(x, y) = \sum_{i=1}^N u(x_i, y_i) \Phi_i(x, y) + \sum_{T \in \mathcal{T}_h^{int}} Q_T \phi_{J,T}(x, y), \quad (2.22)$$

where

$$Q_T = \int_{\Gamma \cap T} Q ds. \quad (2.23)$$

The interpolation (2.22) converges optimally in  $H^1$ - and  $L^2$ - norms based on numerical experiments carried out in [22]. More details about nonhomogeneous IFE methods can be found in [30,22,23].

### 2.4. Galerkin IFE method

In this subsection, we derive the Galerkin IFE methods for solving the interface problem with periodic boundary condition and nonhomogeneous flux jump (2.7)–(2.10). Define the test function space  $V$  by

$$V = \{v \in H^1(\Omega) : v|_{\Gamma_l} = v|_{\Gamma_b} = 0, v|_{\Gamma_l} = v|_{\Gamma_r}\}. \quad (2.24)$$

Multiplying the differential equation (2.7) by any function  $v \in V$ , integrating over each subdomain, applying the Green's formula, and summing over the subdomains, we have

$$\sum_{s=\pm} \int_{\Omega^s} \beta \nabla u \cdot \nabla v dx dy - \sum_{s=\pm} \int_{\partial \Omega^s} \beta \frac{\partial u}{\partial n} v ds = \int_{\Omega} f v dx dy, \quad \forall v \in V.$$

Applying the flux jump condition (2.6) we have

$$\int_{\Omega} \beta \nabla u \cdot \nabla v dx dy - \int_{\partial \Omega} \beta \frac{\partial u}{\partial n} v ds - \int_{\Gamma} Q v ds = \int_{\Omega} f v dx dy, \quad \forall v \in V. \quad (2.25)$$

The second term in (2.25) equals zero because  $u$  satisfies periodic boundary conditions (2.8), and  $v$  is chosen from  $V$ . Hence, (2.25) can be written as

$$\sum_{T \in \mathcal{T}} \int_T \beta \nabla u \cdot \nabla v dx dy = \int_{\Omega} f v dx dy + \int_{\Gamma} Q v ds, \quad \forall v \in V. \quad (2.26)$$

Now we approximate  $u$  by  $u_h \in S_h^{IFE}(\Omega)$ , and approximate  $v$  by  $v_h \in S_h(\Omega)$ , then

$$\sum_{T \in \mathcal{T}_h} \int_T \beta \nabla u_h \cdot \nabla v_h dx dy = \int_{\Omega} f v_h dx dy + \sum_{T \in \mathcal{T}_h^{int}} \int_{\Gamma \cap T} Q v_h ds. \quad (2.27)$$

The structure of interpolation (2.22) indicates that we can decompose the function  $u_h \in S_h^{IFE}(\Omega)$  as follows

$$u_h = \tilde{u}_h + \sum_{T \in \mathcal{T}_h^{int}} Q_T \phi_{J,T} \quad (2.28)$$

where  $Q_T$  can be calculated by (2.23), and  $\tilde{u}_h \in S_h(\Omega)$  satisfying the homogeneous flux jump. The Galerkin IFE method can be formed as: Find  $\tilde{u}_h \in S_h(\Omega)$  such that

$$a(\tilde{u}_h, v_h) = F(v_h), \quad \forall v_h \in S_h(\Omega), \quad (2.29)$$

where

$$a(u, v) = \sum_{T \in \mathcal{T}_h} \int_T \beta \nabla u \cdot \nabla v dx dy, \quad (2.30)$$

$$F(v) = \int_{\Omega} f v dx dy + \sum_{T \in \mathcal{T}_h^{int}} \int_{\Gamma \cap T} Q v ds - \sum_{T \in \mathcal{T}_h^{int}} Q_T \int_T \beta \nabla \phi_{J,T} \cdot \nabla v dx dy. \quad (2.31)$$

Clearly, the solution  $u_h$  and the test function  $v_h \in S_h(\Omega)$  do not necessarily satisfy the PBCs  $u_h|_{\Gamma_l} = u_h|_{\Gamma_r}$  and  $v_h|_{\Gamma_l} = v_h|_{\Gamma_r}$ . Hence, we need to modify the stiffness matrix to incorporate these boundary conditions.

### 3. Matrix modification for PBC

In this section, we introduce a technique to modify the stiffness matrix and right-hand-side vector to handle periodic boundary conditions. The advantage of this technique is that the matrix will preserve the symmetric positive definite property, so that it can be solved efficiently. The main idea of this technique is originated from [34].

The IFE method (2.29) is equivalent to the linear system

$$A\mathbf{u} = \mathbf{b}, \quad (3.1)$$

where  $A = [a_{ij}] = [a(\Phi_i, \Phi_j)]$  is an  $N \times N$  stiffness matrix and it is symmetric positive definite,  $\mathbf{b} = [b_i] = [F(\Phi_i)]$  is an  $N$ -vector, and  $\mathbf{u} = [u_i]$  is the vector of unknowns.

The periodic boundary condition (2.2) indicates that several components of  $\mathbf{u}$  must have the same value. Without loss of generality, we assume that the  $i$ th and  $j$ th ( $j < i$ ) components of  $\mathbf{u}$  satisfy the following periodic relationship

$$u_j = u_i. \quad (3.2)$$

The complete cycle of the matrix modification has two steps. The first step is to enforce the periodic condition (3.2). To do this, we define an elementary matrix  $E_{ij}$  by

$$E_{ij} = \begin{bmatrix} 1 & \cdots & 0 & \cdots & 0 & \cdots & 0 \\ \vdots & \ddots & \vdots & & \vdots & & \vdots \\ 0 & \cdots & 1 & \cdots & 0 & \cdots & 0 \\ \vdots & & \vdots & \ddots & \vdots & & \vdots \\ 0 & \cdots & 1 & \cdots & 1 & \cdots & 0 \\ \vdots & & \vdots & & \vdots & \ddots & \vdots \\ 0 & \cdots & 0 & \cdots & 0 & \cdots & 1 \end{bmatrix} \begin{matrix} \\ \\ \text{jth} \\ \\ \text{ith.} \\ \\ \end{matrix}$$

Multiplying both sides of Eq. (3.1) by  $E_{ij}$ , we obtain an equivalent system

$$(E_{ij}A)\mathbf{u} = E_{ij}\mathbf{b}. \quad (3.3)$$

Now we replace the  $j$ th equation of the system (3.3) by the periodic relationship (3.2), we obtain

$$A_1 \mathbf{u} = \mathbf{b}_1, \quad (3.4)$$

where

$$A_1 = \begin{bmatrix} a_{11} & \cdots & a_{1j} & \cdots & a_{1i} & \cdots & a_{1n} \\ \vdots & \ddots & \vdots & \ddots & \vdots & \ddots & \vdots \\ 0 & \cdots & 1 & \cdots & -1 & \cdots & 0 \\ \vdots & \ddots & \vdots & \ddots & \vdots & \ddots & \vdots \\ a_{i1} + a_{j1} & \cdots & a_{ij} + a_{jj} & \cdots & a_{ii} + a_{ji} & \cdots & a_{in} + a_{jn} \\ \vdots & \ddots & \vdots & \ddots & \vdots & \ddots & \vdots \\ a_{n1} & \cdots & a_{nj} & \cdots & a_{ni} & \cdots & a_{nn} \end{bmatrix} \begin{matrix} \\ \\ j\text{th} \\ \\ ith \\ \\ \end{matrix}$$

and

$$\mathbf{b}_1 = [b_1, \dots, b_{j-1}, 0, b_{j+1}, \dots, b_i + b_j, \dots, b_n]^T.$$

Clearly, the matrix  $A_1$  is not symmetric. In the second step, we correct this matrix to make it symmetric positive definite. Let  $L_{ij}$  be the following matrix

$$L_{ij} = \begin{bmatrix} 1 & \cdots & -a_{1j} & \cdots & 0 & \cdots & 0 \\ \vdots & \ddots & \vdots & \ddots & \vdots & \ddots & \vdots \\ 0 & \cdots & 1 & \cdots & 0 & \cdots & 0 \\ \vdots & \ddots & \vdots & \ddots & \vdots & \ddots & \vdots \\ 0 & \cdots & -(1 + a_{jj}) - a_{ij} & \cdots & 1 & \cdots & 0 \\ \vdots & \ddots & \vdots & \ddots & \vdots & \ddots & \vdots \\ 0 & \cdots & -a_{nj} & \cdots & 0 & \cdots & 1 \end{bmatrix} \begin{matrix} \\ \\ j\text{th} \\ \\ ith \\ \\ \end{matrix}.$$

Multiplying both sides of (3.4) by  $L_{ij}$  yields the following equation:

$$A_2 \mathbf{u} := L_{ij} A_1 \mathbf{u} = L_{ij} \mathbf{b}_1 =: \mathbf{b}_2. \quad (3.5)$$

A straightforward calculation shows that

$$A_2 = \begin{bmatrix} a_{11} & \cdots & 0 & \cdots & a_{1i} + a_{1j} & \cdots & a_{1n} \\ \vdots & \ddots & \vdots & \ddots & \vdots & \ddots & \vdots \\ 0 & \cdots & 1 & \cdots & -1 & \cdots & 0 \\ \vdots & \ddots & \vdots & \ddots & \vdots & \ddots & \vdots \\ a_{i1} + a_{j1} & \cdots & -1 & \cdots & 1 + a_{ii} + a_{jj} + 2a_{ij} & \cdots & a_{in} + a_{jn} \\ \vdots & \ddots & \vdots & \ddots & \vdots & \ddots & \vdots \\ a_{n1} & \cdots & a_{nj} & \cdots & a_{ni} + a_{nj} & \cdots & a_{nn} \end{bmatrix} \begin{matrix} \\ \\ j\text{th} \\ \\ ith \\ \\ \end{matrix}$$

$$\mathbf{b}_2 = [b_1, \dots, b_{j-1}, 0, b_{j+1}, \dots, b_i + b_j, \dots, b_n]^T.$$

One can easily verify that (3.5) removes the periodic relationship of  $u_i$  and  $u_j$  from (3.1). Moreover, the matrix  $A_2$  is symmetric positive definite. We continue this procedure until we go through all nodes with such periodicity.

#### 4. Numerical examples

In this section, we will present several numerical examples to illustrate features of this IFE method for interface problems with periodic boundary condition.

##### 4.1. Field calculation with periodic boundary condition

In this example, we assume that  $\Omega = (-1, 1) \times (-1, 1)$  is an open rectangular domain and  $\mathcal{T}_h$  is a Cartesian mesh of  $\Omega$  whose element size is  $h$ . The interface curves are two semi-circles with radius  $r_0 = \frac{\pi}{6.28}$  that separates  $\Omega$  into three sub-domains  $\Omega_1^- = \{(x, y) : (x - 1)^2 + y^2 < r_0^2\}$ ,  $\Omega_2^- = \{(x, y) : (x + 1)^2 + y^2 < r_0^2\}$  and  $\Omega^+ = \Omega - \overline{\Omega_1^-} \cup \overline{\Omega_2^-}$ . Two interfaces are defined as  $\Gamma_1 = \overline{\Omega^+} \cap \overline{\Omega_1^-}$ , and  $\Gamma_2 = \overline{\Omega^+} \cap \overline{\Omega_2^-}$ . The simulation domain is illustrated in Fig. 1.

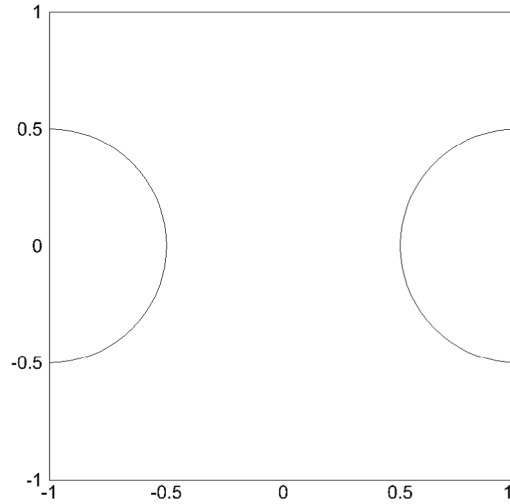


Fig. 1. Simulation domain  $\Omega$  for Example 4.1.

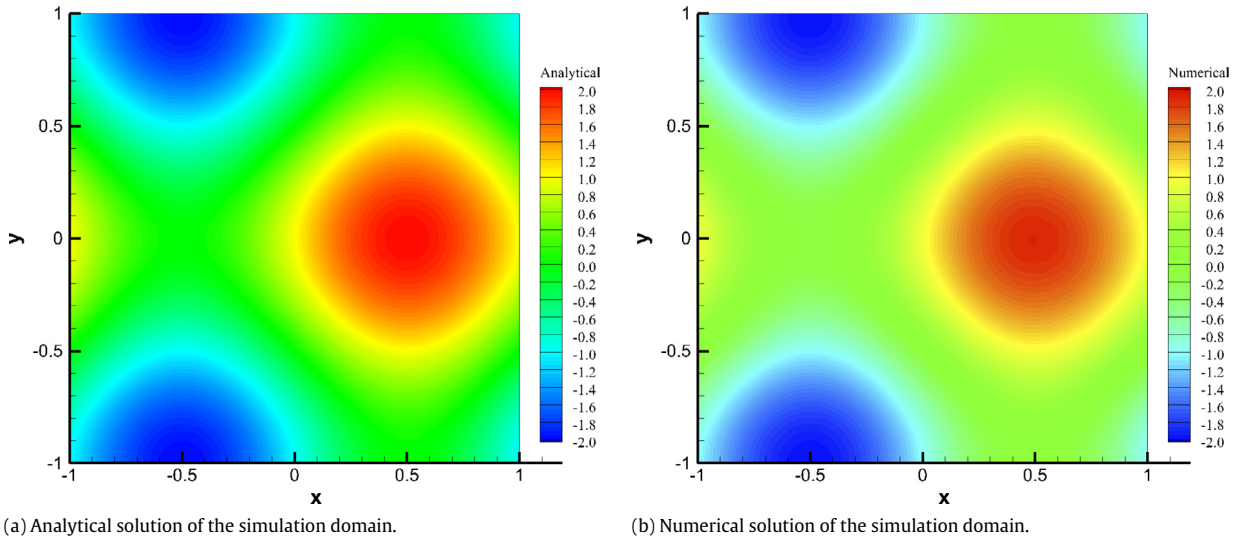


Fig. 2. Analytical solution and numerical solution for Example 4.1.

Let the exact solution of the potential be

$$u(x, y) = \sin(\pi x) + \cos(\pi y) \quad (4.1)$$

with  $\beta_1^- = \beta_2^- = 1$ ,  $\beta^+ = 10$ . We note that  $u$  satisfies the following jump conditions across two interfaces  $\Gamma_1$  and  $\Gamma_2$ :

$$\begin{aligned} \llbracket u \rrbracket_{\Gamma_1} &= \llbracket u \rrbracket_{\Gamma_2} = 0, \\ \left[ \left[ \beta \frac{\partial u}{\partial n} \right] \right]_{\Gamma_1} &= Q_1(x, y) = (\beta^+ - \beta_1^-) \frac{\pi(x-1) \cos(\pi x) - \pi y \sin(\pi y)}{\sqrt{(x-1)^2 + y^2}}, \\ \left[ \left[ \beta \frac{\partial u}{\partial n} \right] \right]_{\Gamma_2} &= Q_2(x, y) = (\beta^+ - \beta_2^-) \frac{\pi(x+1) \cos(\pi x) - \pi y \sin(\pi y)}{\sqrt{(x+1)^2 + y^2}}. \end{aligned}$$

Periodic boundary conditions (2.3) and (2.4) are imposed on the left and right boundaries. The Dirichlet boundary condition (2.2) is imposed on the upper and lower boundaries. Fig. 2(a) and (b) show the analytical and numerical solutions of this problem, respectively. These plots are generated on a Cartesian mesh of size  $h = 1/32$ . Comparing the numerical solution with exact solution, we can see that the IFE method can recover the solution accurately.

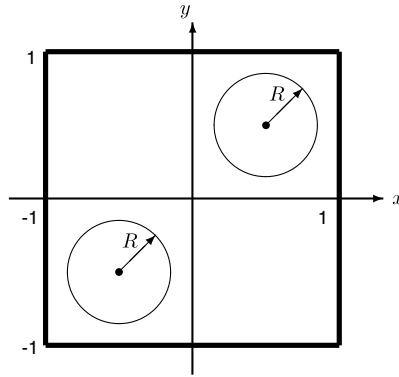


Fig. 3. Simulation domain  $\Omega$  in Example 4.2.

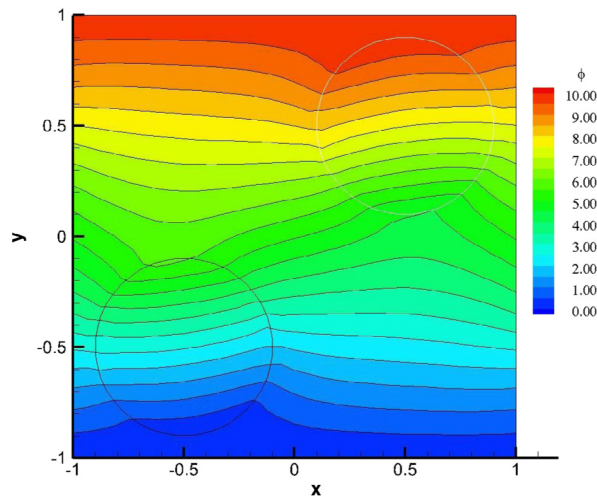


Fig. 4. IFE solution for conducting cylinders with PBC.

#### 4.2. Dielectric cylinders with periodic boundary

In this example, we simulate the electrical field around dielectric cylinders with periodic boundary. The 2-D simulation domain  $\Omega = (-1, 1) \times (-1, 1)$  is shown in Fig. 3. Two dielectric cylinders with radius  $R = 0.4002$  locate in the domain whose centers are  $(-0.5, -0.5)$  and  $(0.5, 0.5)$ , respectively. We apply the periodic boundary conditions on the left and right boundaries. The top and bottom boundaries are set to be Dirichlet type boundaries with  $u = 10$  and  $u = 0$  respectively. The coefficient  $\beta$  is set to be 1 inside the dielectric cylinders and to be 10 outside. The exact solution of this example is unknown.

In our numerical simulation, the mesh size is set to be  $h = 1/16$  and the background charge density is set to be  $f = 1$ . The flux jump is  $-10$  on left half of every dielectric cylinder, and  $10$  on the right half. Fig. 4 shows the numerical solution of the potential distribution using the IFE method. Fig. 5 is a duplicated plot of three simulation domains. On the combining boundaries  $x = -1$  and  $x = 1$ , the potential is well matched for the periodic structures.

#### 4.3. Further discussion about IFE methods

The IFE method (2.29) is based on classical Galerkin formulation. For Example 4.1, we observe that the order of convergence in either  $L^2$  or  $H^1$ - norm is only sub-optimal. The convergence order varies according to the location of interface and the jump ratio of coefficient. Actually, it was recently reported in [17] that the order of convergence may deteriorate for interface problems with pure Dirichlet boundary condition and homogeneous flux jump ( $Q = 0$ ). It is not surprising that the order of convergence cannot attain optimal for this more complicated problem with periodic boundary conditions.

In [17,14], some partially penalized IFE schemes have been developed and analyzed for elliptic interface problems with homogeneous flux jump. These new IFE schemes are more accurate and optimal convergence can be theoretically proved. It will be an interesting future work to extend these new IFE schemes in [14,17] to nonhomogeneous flux jump case, and other boundary conditions such as PBC.

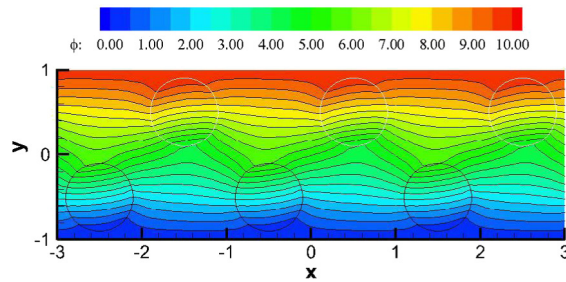


Fig. 5. IFE solution for conducting cylinders on three simulation domains.

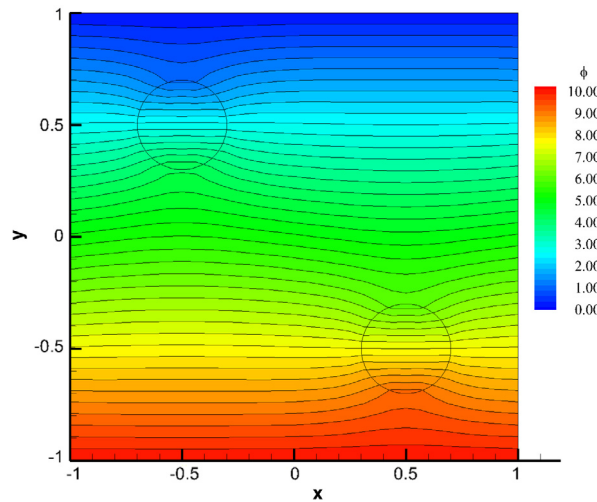


Fig. 6. Symmetric partially penalized IFE solution for conducting cylinders with homogeneous flux jump.

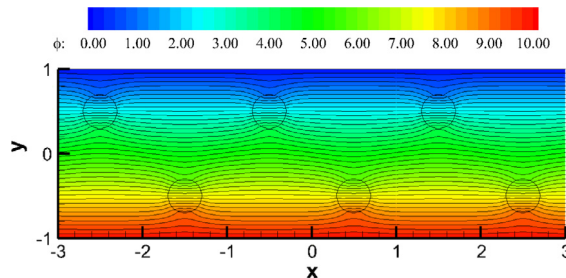


Fig. 7. Symmetric partially penalized IFE solution for conducting cylinders homogeneous flux jump on three simulation domains.

For a preliminary test with homogeneous flux jump  $Q = 0$ , we report some numerical result for the symmetric partial penalized IFE scheme in [17] with PBC. Two dielectric cylinders with radius  $R = 0.2002$  are located in the domain whose centers are  $(-0.5, 0.5)$  and  $(0.5, -0.5)$ . The charging density  $f = 1$ . On the top and bottom boundaries, we impose Dirichlet boundary conditions  $u = 0$ , and  $u = 10$ , respectively. On the left and right boundaries, the periodic boundary conditions are enforced. Figs. 6 and 7 report the numerical solution of the potential distribution, and a combined plot of three simulation domains. Since the exact solution is unknown in this case, we cannot test the order of convergence at this moment.

## 5. Conclusions

In this paper, we present an IFE method for an unbounded elliptic interface problem with periodic structure. The problem can be reformulated in a finite domain with appropriate periodic boundary conditions. The periodic boundary conditions can be accommodated by modifying the stiffness matrix, whose symmetric positive definite structure can be preserved. We use several numerical experiments to demonstrate the effectiveness of our new IFE algorithm.

## References

- [1] R. Kafafy, Immersed finite element particle-in-cell simulations of ion propulsion (Ph.D. thesis), Virginia Polytechnic Institute and State University, USA, 2005.
- [2] J. Wang, Y. Cao, R. Kafafy, R. Martinez, J. Williams, Numerical and experimental investigations of crossover ion impingement for subscale ion optics, *J. Propul. Power* 24 (3) (2008) 562–570.
- [3] A. Bergmann, Two-dimensional particle simulation of langmuir probe sheaths with oblique magnetic field, *Phys. Plasmas* 1 (1994) 3598.
- [4] K. Matyash, R. Schneider, Finite size effects on charging in dusty plasmas, *J. Plasma Phys.* 72 (6) (2006) 809–812.
- [5] K. Matyash, R. Schneider, R. Sydora, F. Taccogna, Application of a grid-free kinetic model to the collisionless sheath, *Contrib. Plasma Phys.* 48 (1–3) (2008) 116–120.
- [6] X. Xu, G. DiPeso, V. Vahedi, C. Birdsall, Theory and simulation of plasma sheath waves. Technical report, California Univ, Berkeley, CA, United States, Electronics Research Lab, 1992.
- [7] Y. Cao, Y. Chu, X. He, T. Lin, An iterative immersed finite element method for an electric potential interface problem based on given surface electric quantity, *J. Comput. Phys.* 281 (2015) 82–95.
- [8] Y. Chu, Y. Cao, X. He, M. Luo, Asymptotic boundary conditions with immersed finite elements for interface magnetostatic/electrostatic field problems with open boundary, *Comput. Phys. Comm.* 182 (11) (2011) 2331–2338.
- [9] R. Kafafy, T. Lin, Y. Lin, J. Wang, Three-dimensional immersed finite element methods for electric field simulation in composite materials, *Internat. J. Numer. Methods Engrg.* 64 (7) (2005) 940–972.
- [10] R. Kafafy, J. Wang, T. Lin, A hybrid-grid immersed-finite-element particle-in-cell simulation model of ion optics plasma dynamics, *Dyn. Contin. Discrete Impuls. Syst. Ser. B Appl. Algorithms* 12 (2005) 1–16.
- [11] R. Kafafy, J. Wang, A hybrid grid immersed finite element particle-in-cell algorithm for modeling spacecraft–plasma interactions, *IEEE Trans. Plasma Sci.* 34 (5) (2006) 2114–2124.
- [12] J. Wang, X. He, Y. Cao, Modeling electrostatic levitation of dust particles on lunar surface, *IEEE Trans. Plasma Sci.* 36 (5) (2008) 2459–2466.
- [13] W. Feng, X.-M. He, Y. Lin, X. Zhang, Immersed finite element method for interface problems with algebraic multigrid solver, *Commun. Comput. Phys.* 15 (4) (2014) 228–247.
- [14] J. Guzman, M.A. Sanchez, M. Sarkis, A finite element method for high-contrast interface problems with error estimates independent of contrast, 2015, arXiv:1507.03873.
- [15] X. He, T. Lin, Y. Lin, A selective immersed discontinuous Galerkin method for elliptic interface problems, *Math. Methods Appl. Sci.* 37 (7) (2014) 983–1002.
- [16] Z. Li, The immersed interface method using a finite element formulation, *Appl. Numer. Math.* 27 (3) (1997) 253–267.
- [17] T. Lin, Y. Lin, X. Zhang, Partially penalized immersed finite element methods for elliptic interface problems, *SIAM J. Numer. Anal.* 53 (2) (2015) 1121–1144.
- [18] T. Lin, D. Sheen, X. Zhang, A locking-free immersed finite element method for planar elasticity interface problems, *J. Comput. Phys.* 247 (2013) 228–247.
- [19] T. Lin, Q. Yang, X. Zhang, A priori error estimates for some discontinuous Galerkin immersed finite element methods, *J. Sci. Comput.* 65 (3) (2015) 875–894.
- [20] S.A. Sauter, R. Warnke, Composite finite elements for elliptic boundary value problems with discontinuous coefficients, *Computing* 77 (1) (2006) 29–55.
- [21] Y. Gong, B. Li, Z. Li, Immersed-interface finite-element methods for elliptic interface problems with non-homogeneous jump conditions, *SIAM J. Numer. Anal.* 46 (2008) 472–495.
- [22] X. He, T. Lin, Y. Lin, Immersed finite element methods for elliptic interface problems with non-homogeneous jump conditions, *Int. J. Numer. Anal. Model.* 8 (2) (2011) 284–301.
- [23] T. Lin, Y. Lin, X. Zhang, Immersed finite element method of lines for moving interface problems with nonhomogeneous flux jump, in: *Recent Advances in Scientific Computing and Applications*, in: *Contemp. Math.*, vol. 586, Amer. Math. Soc., Providence, RI, 2013, pp. 257–265.
- [24] K.S. Chang, D.Y. Kwak, Discontinuous bubble scheme for elliptic problems with jumps in the solution, *Comput. Methods Appl. Mech. Engrg.* 200 (5–8) (2011) 494–508.
- [25] X. He, T. Lin, Y. Lin, Approximation capability of a bilinear immersed finite element space, *Numer. Methods Partial Differential Equations* 24 (5) (2008) 1265–1300.
- [26] Z. Li, T. Lin, Y. Lin, R.C. Rogers, An immersed finite element space and its approximation capability, *Numer. Methods Partial Differential Equations* 20 (3) (2004) 338–367.
- [27] Z. Li, T. Lin, X. Wu, New Cartesian grid methods for interface problems using the finite element formulation, *Numer. Math.* 96 (1) (2003) 61–98.
- [28] K. Vemaganti, Discontinuous Galerkin methods for periodic boundary value problems, *Numer. Methods Partial Differential Equations* 23 (3) (2007) 587–596.
- [29] T. Lin, Y. Lin, R. Rogers, M.L. Ryan, A rectangular immersed finite element space for interface problems, in: *Scientific Computing and Applications*, Kananaskis, AB, 2000, in: *Adv. Comput. Theory Pract.*, vol. 7, Nova Sci. Publ., Huntington, NY, 2001, pp. 107–114.
- [30] X. He, Bilinear immersed finite elements for interface problems (Ph.D. thesis), Virginia Polytechnic Institute and State University, USA, 2009.
- [31] X. He, T. Lin, Y. Lin, The convergence of the bilinear and linear immersed finite element solutions to interface problems, *Numer. Methods Partial Differential Equations* 28 (1) (2012) 312–330.
- [32] T. Lin, Y. Lin, R.C. Rogers, L.M. Ryan, A rectangular immersed finite element method for interface problems, in: P. Mineev, Y. Lin (Eds.), *Advances in Computation: Theory and Practice*, Vol. 7, Nova Science Publishers, Inc., 2001, pp. 107–114.
- [33] T. Lin, X. Zhang, Linear and bilinear immersed finite elements for planar elasticity interface problems, *J. Comput. Appl. Math.* 236 (18) (2012) 4681–4699.
- [34] A. Huang, A method for treating periodical boundary condition, *J. Numer. Methods Comput. Appl.* 4 (1) (1983) 37–46.